

04/15/2003

LA-UR-03-2521

Approved for public release;
distribution is unlimited.

42

Title: ASME CODE DUCTILE FAILURE CRITERIA FOR
IMPULSIVELY LOADED PRESSURE VESSELS

Author(s): Robert E. Nickell
Thomas A. Duffey
Edward A. Rodriguez

Submitted to: 2003 ASME Pressure Vessels and Piping Conference
Cleveland, OH USA



Los Alamos National Laboratory, an affirmative action/equal opportunity employer, is operated by the University of California for the U.S. Department of Energy under contract W-7405-ENG-36. By acceptance of this article, the publisher recognizes that the U.S. Government retains a nonexclusive, royalty-free license to publish or reproduce the published form of this contribution, or to allow others to do so, for U.S. Government purposes. Los Alamos National Laboratory requests that the publisher identify this article as work performed under the auspices of the U.S. Department of Energy. Los Alamos National Laboratory strongly supports academic freedom and a researcher's right to publish; as an institution, however, the Laboratory does not endorse the viewpoint of a publication or guarantee its technical correctness.

ASME Code Ductile Failure Criteria for Impulsively Loaded Pressure Vessels

Robert E. Nickell
Applied Science & Technology
16630 Sagewood Lane
Poway, CA 92064 USA
RNickell@cox.net

Thomas A. Duffey
Consulting Engineer
P. O. Box 1239
Tijeras, NM 87059 USA
TDuffey2@aol.com

Edward A. Rodriguez
Los Alamos National Laboratory
Mail Stop P946
Los Alamos, NM 87545 USA
ERodriguez@lanl.gov

ABSTRACT

Ductile failure criteria suitable for application to impulsively loaded high pressure vessels that are designed to the rules of the ASME Code Section VIII Division 3 are described and justified. The criteria are based upon prevention of load instability and the associated global failure mechanisms, and on protection against progressive distortion for multiple-use vessels. The criteria are demonstrated by the design and analysis of vessels that contain high explosive charges.

BACKGROUND

Ductile failure design methodologies for high explosive (HE) detonation-induced impulse loading in pressure vessels are presented herein. Typical pressure vessel systems are shown in Figure 1 and Figure 2. One previous Los Alamos National Laboratory (LANL) design, shown in Figure 1, consists of a 6-ft (1.83-m) inside diameter containment vessel with three access ports. The HE charge is placed inside the vessel at the geometric center of the spherical shell. The United Kingdom Atomic Weapons Establishment (AWE) design, shown in Figure 2, consists of a cylindrical vessel with a hemispherical end-cap and a heavy reinforcement closure connection.

A pressure vessel under internal HE detonation is typically subjected to two distinct types of loading. First, immediately following detonation of the HE, the shock wave inside the vessel imparts a transient impulsive pressure loading to the vessel wall. Second, a long-term quasi-static pressure buildup occurs in the vessel as a result of expanding reaction gas products. It is the early-time impulsive loading that is limiting for containment vessel design. In order to ensure the containment function for the vessel materials of construction, the designer must start with rational ductile failure design criteria that utilize the plastic reserve capacity to provide an appropriate structural margin.

The following sections describe such rational ductile failure design criteria, both for single-use and multiple-use vessels. Section 2 of this paper briefly describes detonation loading in a containment vessel; however, the bulk of the discussion of the detonation loading

function is contained in Reference 1, to be published in a Welding Research Council bulletin. Then, Section 3 provides a discussion of ASME Code principles that should be used to develop ductile failure criteria and limits, followed by a brief description in Section 4 of the AWE pressure vessel design methodology for detonation loading for multiple-use vessels [2a, 2b]. This work will be published in greater

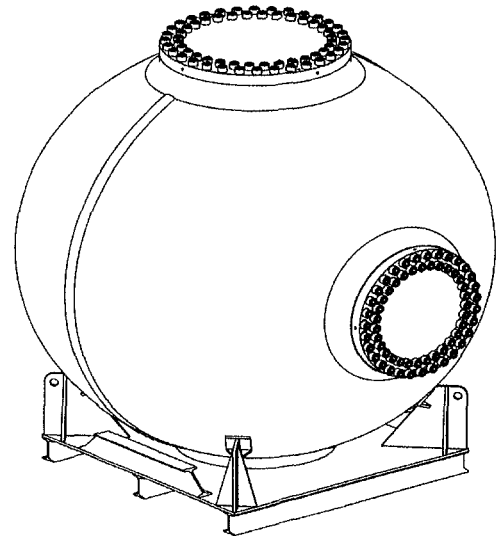


Figure 1. Single-Use LANL Containment Vessel

detail in a subsequent Welding Research Council bulletin. Then, Section 5 describes the LANL design criteria and methodology specifically developed for single-use vessels for HE detonation. Section 5 follows up on the plastic tensile instability criteria discussed in Section 3, together with the results of the application of ASME Code collapse methodology as applied to the LANL containment vessel. Finally, Section 5 describes load-controlled

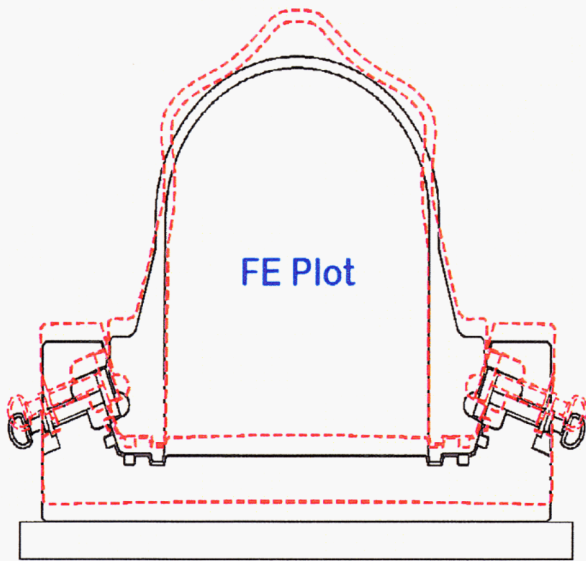


Figure 2. Multiple-Use AWE Containment Vessel with Deformed Shape Plot

versus energy-controlled structural limits critical to the discussion of design criteria for detonation-induced vessel response, and introduces ductile tearing initiation methodology, followed by the proposed allowable strain limits for detonation-induced loading for single-use vessels. A summary is provided in Section 6.

2. HIGH EXPLOSIVE DETONATION LOADING

One of the main differences between pressure vessels loaded statically and containment vessels loaded explosively is the characteristic of dynamic structural response. For containment vessels loaded explosively, the shock reflects from the vessel wall and undergoes a number of additional reflections as it decays. These subsequent reflections are generally of reduced magnitude, so they usually do not induce significant additional vibrations. The reflected pressure and the impulse of the initial shock can be calculated from free air blast curves, such as those given by Baker [3], that show the normalized pressure and impulse as a function of the normalized distance from the explosive charge – distance/(charge weight)^{1/3}. These curves have been found to agree well with values obtained from detailed hydrodynamics calculations that model the detonation and subsequent shocks. Where subsequent shocks are important, full hydrodynamic analysis is now common.

The vessel response depends upon the duration of the pressure pulse compared to the natural vibration periods of the vessel walls. If the shock duration is much shorter than the fundamental vibration period, the key factor is the impulse, and peak pressure is not as important. If the shock duration is much longer than the fundamental vibration period, then the peak pressure controls the response amplitude. In most cases, the structural response of high explosive (HE) blast loaded containment vessels is controlled by the shock impulse, rather than by the shock peak pressure. Therefore, a maximum pressure limitation on the vessel, as is common for statically-loaded vessels, is not meaningful. However, peak pressure does play an important role in deflagration events, as described by Duffey, et al. [1].

3. BACKGROUND

3.1 ASME Code Ductile Failure Mode Background

The fundamental starting point for ASME Code rules [4a] is the definition of the failure mode under consideration and the identification of the controlling parameter(s). In this case, the principal failure mode under consideration is ductile rupture, which includes sub-categories such as plastic instability (e.g., the inability of the structure or vessel to maintain its geometry and therefore its load-carrying or pressure-retaining function) and local ductile tearing. For the purposes of this discussion, one additional failure mode will be included -- buckling instability. For static or quasi-static loading, buckling instability is defined as the coexistence of dual equilibrium states. However, for dynamic loading, dynamic buckling instability is defined (see Reference 5) as the condition of dynamic stress and deformation in time such that at least one instantaneous eigenvalue of the structural system vanishes. This same principle applies to dynamic plastic instability. The structural system, whether described continuously (in closed form) or discretely (e.g., finite element model), undergoes a state of stress and deformation in time such that at least one eigenvalue of the nonlinear structural system vanishes.

For static or quasi-static loading conditions, one method for determining collapse load is given in Appendix II of Section III, Division 1, *Experimental Stress Analysis*, Paragraph II-1430 [4b]. The collapse load methodology is based on obtaining a load-deflection characteristic similar to that shown in Figure 3.

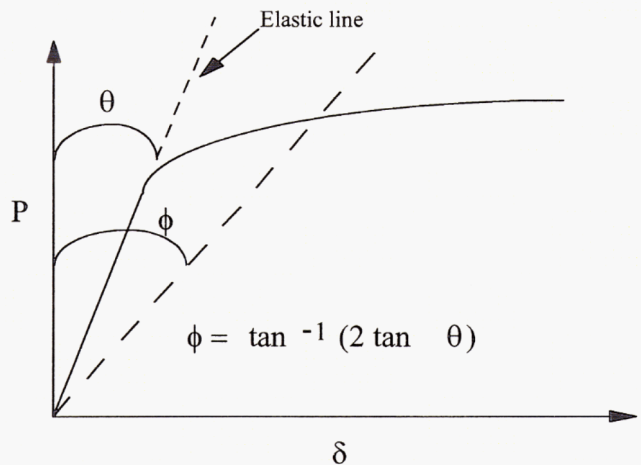


Figure 3. Load-Deflection Characteristic For Static Collapse

Appendix F of Section III requires that only one of the five listed methods (elastic analysis, plastic analysis, collapse load analysis, plastic instability analysis, and interaction method) need be used to demonstrate acceptability. Here we have used the Plastic Instability Load method as the preferred approach, using strain limits rather than a limit on the instability load, P_I , itself. The Plastic Instability Load is defined in NB-3213.26. That definition was developed carefully by the ASME Code bodies, as described by Gerdeen in a Welding Research Council (WRC) Bulletin [6]. The Plastic Instability Load corresponds to the Plastic Instability Pressure for pressure vessels. Plastic instability in this case is defined to be the point on the

pressure-deflection curve with a zero slope, generally obtained from elastic-plastic, large deflection analysis. Note that Gerdeen states clearly that

“Plastic instability in this case is not a material instability such as ‘necking’ in simple tension, but a structural instability resulting from a combination of compressive hoop stresses and plastic yielding.”

Therefore, the nomenclature used in Appendix F of Section III of the ASME Code is consistent with the nomenclature used in Appendix II of Section III, and is intended to prevent large deformations caused by a structural instability (e.g., a zero slope on the load-deflection curve that implies zero stiffness).

Following definition of the plastic instability ductile failure mode, the next ASME Code principle to be examined is the identification of the controlling parameter(s). For static and quasi-static loading, stress is generally considered to be the controlling parameter for both ductile rupture and buckling. However, a close examination of the design-by-analysis rules shows that this is an oversimplification. The stresses must be considered simultaneously with knowledge of the **failure mechanism**.

Consider the case of a flat head on a cylindrical pressure vessel. The tensile membrane stresses that are in equilibrium with the internal pressure are parameters that partially control ductile rupture. However, the discontinuity bending stresses at the cylinder-head junction are not considered primary stresses (parameters that partially control ductile rupture) unless margin against a plastic collapse failure mechanism is insufficient. That is, if the primary bending stress at the center of the head provides sufficient margin against a plastic collapse failure mechanism, the discontinuity bending stresses may be considered to be secondary stresses (parameters that control distortion, but not ductile rupture).

Gerdeen [6] describes a number of alternate “plastic instability pressures” that could be used to define pressure vessel ductile failure, including Limit Pressure as calculated from rigid perfectly-plastic theory. All would provide protection against the zero stiffness associated with Figure 3. Others include the Tangent-Intersection Pressure, the 1 % Plastic Strain Pressure, the Twice-Elastic-Deformation Pressure, and the 0.2 % Offset Strain Pressure. This latter plastic pressure is defined in the ASME Code Section VIII as the pressure that causes a permanent strain of 0.2 % at the location of maximum strain. This strain is a bending strain, however, not a membrane strain.

Gerdeen described two other relevant concepts in Reference 6. First, the bending strain at a plastic hinge is theoretically infinite. However, for real materials with strain hardening and structures with geometrical strengthening, typical yield hinge strains are of the order of 0.6 % or so. Gerdeen also points out that the circumferential membrane strain provides an extremely accurate measure of plastic instability load, since it is proportional to the radial displacement that would be unbounded at the most sensitive location. This last point is a very important factor when considering strain limits as the basis for protection against the plastic instability load.

The principles described above also apply to vessels subjected to dynamic loads. In this case, the dynamic loads are resisted by a combination of inertia and stress that will change as a function of time. The example of the cylindrical vessel with the flat head is

instructive. The membrane stresses resisting an impulsive internal pressure are not tensile at all times, and equilibrium is maintained with a combination of the membrane stresses and inertial forces. However, the fundamental principle of the ductile failure mechanism remains valid. It is possible that, in addition to the discontinuity bending stresses, at least some of the membrane stresses could be considered as secondary if margin against plastic collapse for the entire structure can be demonstrated. For the relatively simple case of the cylindrical pressure vessel with a flat head, the reclassification of some membrane stresses from the primary category to the secondary category might not be worth the effort. However, the calculation of margin against plastic collapse represented by the bending stress at the center of the flat head and at the junctions with the cylindrical wall, including inertial effects, continues to be the design issue.

This ductile failure principle is in common use for evaluating structures subject to impulse loads (see Reference 7). Reference 7 shows that, for frame structures, it is possible to avoid the classification of stress entirely, concentrating on establishing a margin against the plastic collapse load through direct examination of displacements. Gerdeen implied such a procedure in Reference 6 for pressure vessels, based on establishing margin on circumferential strain that is proportional to the critical radial displacement. The same principle would apply to a complex pressure vessel under internal impulsive pressure. Unlike simple frame structures with simple impulsive loading conditions, the plastic hinges that form in more complex pressure vessels under internal impulsive pressure loading will not be stationary, instead traveling from one location to another during the dynamic response.

3.2 Collapse Load for LANL Containment Vessel

A very high static or quasi-static internal pressure could lead to excessive gross yielding, resulting in development of an unstable plastic collapse mechanism. This is shown in Figures 6 and 7, which depict a plastic collapse analysis of the spherical vessel using a 2-D axisymmetric numerical model, shown in Figures 4 and 5. The graph of Figure 6 represents the pressure versus displacement at a critical location in the vessel where unstable plastic collapse occurs. For the model, the collapse location is the vessel’s south pole.

The corresponding behavior represented in Figure 6, i.e., load-deflection, is similar to that shown in Figure 3, resulting in a plastic collapse load (i.e., pressure) of 12,200 psi. This is a numerical calculation performed on a two-dimensional, axisymmetric representation of the vessel using the general purpose, nonlinear finite element code ABAQUS/Standard [8]. Comparison of ASME Code, Section III, Appendix F guidance (with Appendix II rules) for the plastic collapse load limit, Figure 7, shows the overall static collapse load for the vessel is ~11,400 psi internal pressure. This is based on the construction of a line, passing through the plastic portion of the curve, at an angle ϕ from the vertical axis. This internal pressure is well above the long-term quasi-static residual pressure of 1000 psig resulting from the 40-lb HE charge in the containment vessel.

It should be noted however, that this calculation is based on a static internal pressure, not a dynamic event, such as an impulse load generated from HE detonation.



Figure 4 - ABAQUS FEA Model

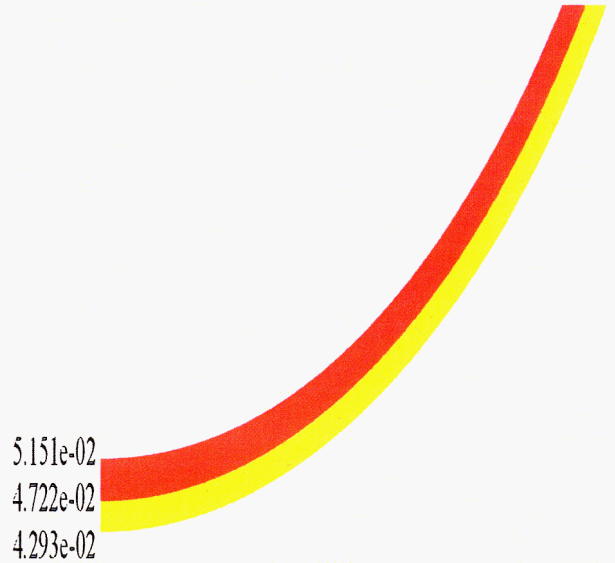


Figure 5. ABAQUS FEA Model – Detail

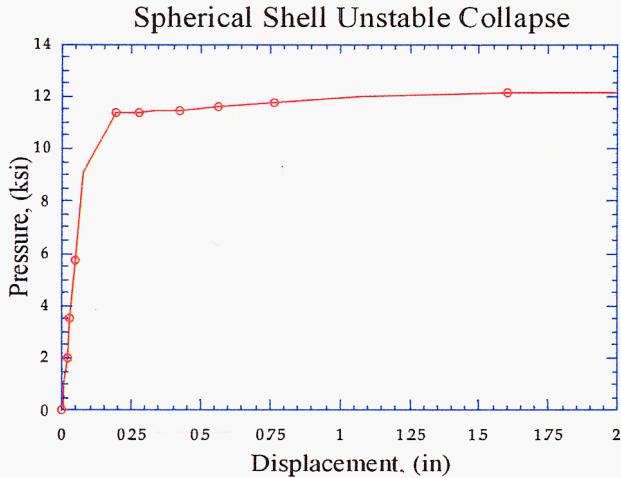


Figure 6. Spherical Shell Static Load-Deflection Curve

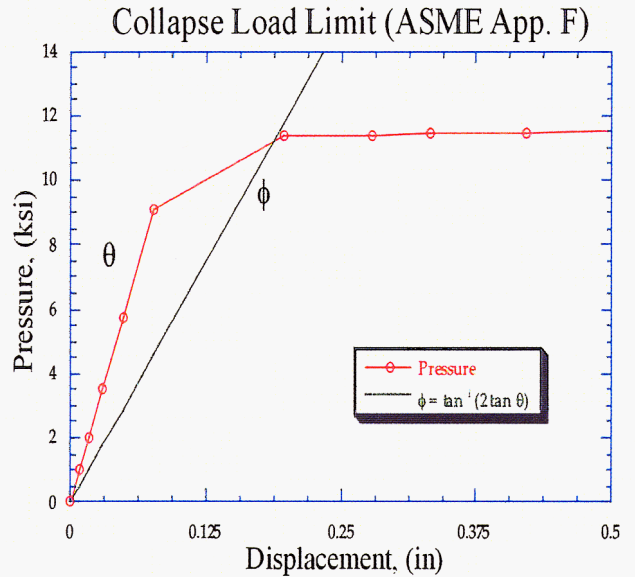


Figure 7. Collapse Load Limit (per ASME Section III, Division 1, Appendix F)

3.3. Direct Dynamic Calculation of Load and Deformation Instability

The most straightforward option would be to carry out dynamic, nonlinear finite element calculations, interrupting the calculations occasionally to calculate the lowest instantaneous frequencies and mode shapes of the nonlinear system. This method has been referred to as the “freeze in time” method (see Reference 9). The nonlinear dynamic analysis is “frozen” in time for a subsidiary calculation intended to show that there are no frequencies approaching a zero frequency and no associated mode shapes approximating plastic instability. Unfortunately, a quantitative margin cannot be determined directly because of the very nature of the failure mechanism – a sudden change from stable to unstable conditions.

Reference 9 describes a slightly modified version of the “freeze in time” method that overcomes this shortcoming. The nonlinear finite element analysis is temporarily halted at points in time where potentially maximum conditions (e.g., high radial displacements,

high accelerations or decelerations) are observed. The forces that exist at those points in time, including the d’Alembert inertial forces, are then increased by a factor until the nonlinear stiffness matrix becomes singular, implying structural instability. That calculated factor should be greater than the margins required for either expected loads or unexpected, but design-basis, loads.

Reference 9 applied this modified procedure only to dynamic buckling caused by impact loads. The method is approximate, with excellent accuracy when the current state of the structure is near structural instability and less accurate when the structure has large margins against instability (e.g., the factor is 10 or more).

4. CRITERIA FOR STRESS-BASED LIMITS

The Atomic Weapons Establishment (AWE) of the United Kingdom has recommended an approach for addressing ductile rupture in confinement vessels subjected to impulsive internal pressure and potential multiple applications. The approach is described, in part, in References 2a and 2b. Those references state that:

“The elastic limit is used in ASME codes conservatively, but it is actually based on the formation of a plastic hinge through the wall at a discontinuity. stresses at local discontinuities can be greater than the elastic limit as long as there is no gross distortion. Where bending stresses and membrane stresses are in phase this is the plastic hinge condition; where membrane stresses remain in one direction during a reversed cycle of bending stresses a ratcheting limit arises. This is where mid thickness stresses must remain elastic during the whole cycle. As this is always more limiting than the plastic hinge condition, this limit is recommended for containment vessels.”

As stated above, the ASME Code rules do not necessarily attempt to prevent plastic hinges from forming, provided that margin against a **plastic hinge failure mechanism** can be demonstrated. As a result, the AWE criteria appear to be very conservative. However, the criteria are intended to protect the vessel from failure during multiple applications, so that the neutral axis must remain elastic to protect against excessive distortion and low-cycle fatigue.

The AWE approach is a stress-based approach that prevents combinations of bending and membrane stress from:

- Forming a plastic hinge at a discontinuity or at any other location in the vessel when the bending and membrane stresses are in phase; or
- Causing excessive distortion (ratcheting) when the bending and membrane stresses are not in phase; and violating elastic behavior at the neutral axis; or
- Causing excessive distortion (ratcheting) when the bending and membrane stresses are not in phase; or
- Violating elastic behavior at the neutral axis.

No plastic hinges are permitted to form at any location in the containment vessel by the AWE approach, even when no plastic hinge failure mechanism (e.g., a combination of plastic hinges leading to plastic instability) is imminent. Ratcheting is not permitted when dynamic loading/unloading cycles are generated. Finally, an even more limiting condition is imposed on the containment vessel – the mid thickness stresses must remain elastic. The neutral axis is protected by requiring a region of elastic behavior (sometimes referred to as an elastic core) at or near the neutral axis for meridional and circumferential bending of the containment vessel.

This option is relatively simple to calculate and enforce, but is very conservative relative to the real concern about plastic instability load.

5. PROPOSED CRITERIA: STRAIN LIMITS

Appendix B of Reference 10 provides design criteria for the high-strength, low-alloy ferritic steel inner confinement vessel of the LANL DynEx Project containment system. These criteria include modifications to the stress-based criteria in the non-mandatory

Appendix F [4] to specifically add membrane and peak strain limits, in lieu of those stress limits. Justification for the strain limits is provided in the following sub-sections.

5.1 Impulse-Driven Structural Response

The allowable strain limits presented later were developed to address the fact that ASME Code stress classification of primary, secondary, and peak stresses is not appropriate in assessing the overall state-of-strain in a dynamically loaded vessel from a detonation shock wave causing high strain-rate effects. Furthermore, there are no “primary stresses” that would cause ductile rupture in the vessel, except for the long-term residual quasi-static overpressure from the reaction gas products. The only Code-type stress that can be attributed as “primary” is the membrane stress from the residual overpressure. As will be shown in this section, the response of the vessel, and the stresses/strains developed in the shell, are based primarily on energy-controlled effects.

Figure 8 shows a pressure-time history for a 40-lb HE charge, center detonated, in a spherical vessel. The detonation event begins at time, $T = 0$ and the pressure pulse reaches the wall at $T = 200 \mu\text{sec}$, which is the first instance the vessel wall is subjected to a loading. Reaction product expansion and collapse is evident from the decaying pressure peaks. At time $T = 1000 \mu\text{sec}$, the initial impulse has largely been delivered to the wall. At this time, the pressure transient has decayed from a peak of about 12,000 psi to about 1,000 psi, in about 800 μsec .

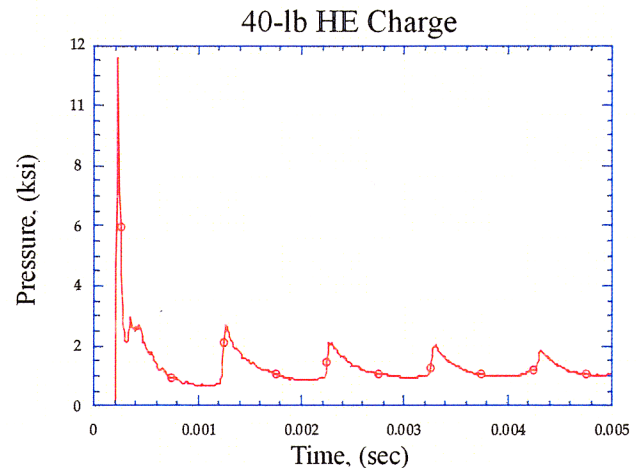


Figure 8. Pressure-Time History For 40-lb HE Detonation (5-ms)

Figure 9 depicts a shortened time scale of the same P-T history to 1 msec. The important factor is the actual time that the vessel is subjected to an overpressure greater than the quasi-static pressure, i.e., 800 μsec . The implication is that from a Code stress classification standpoint, there are no “primary” stresses at peak response, as the peak response is reached at a time well beyond the 800 μsec time limit, as shown in Figures 10 through 12.

As has been discussed by Duffey, et al. [1], it is not peak pressure but rather impulse that provides the driving energy for vessel response. The impulse can be thought as an initial condition on velocity applied to the shell wall. Again, at the point of peak vessel response, the pressure load is minimal and hence there is no significant primary

stress. The stresses must be classified as deformation-controlled, i.e., “secondary,” or as will be discussed later, “energy-controlled.”

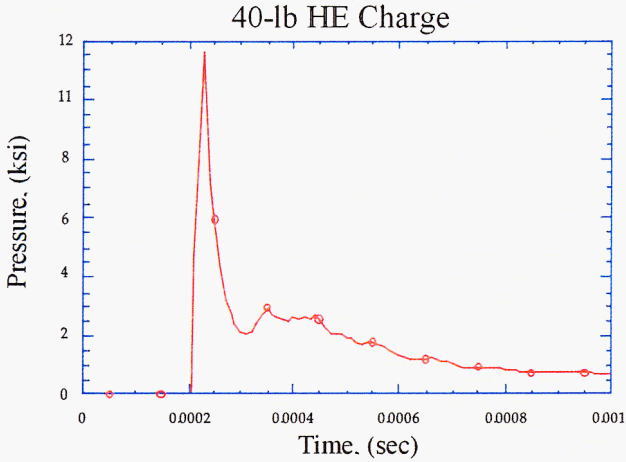


Figure 9. Pressure-Time History For 40-lb HE Detonation (1-ms)

Figures 10 and 11 show the calculated vessel response to the 40-lb HE detonation impulse loading. Response is monitored at numerous vessel locations, yet this particular location is for the South Pole of the vessel. The time sequences are similar to those for the pressure-time histories in Figures 8 and 9. Figure 10 shows that the first mode (i.e., breathing mode of vessel) response peaks at about 0.5-msec. However, the peak vessel response, i.e., maximum stress or strain, does not occur until much later in time at about 6-ms, as shown in Figure 11. Figure 12 shows the pressure-time history superimposed on the maximum stress/strain history, illustrating conclusively that the total impulse, rather than the pressure magnitude itself, that drives the dynamic structural response.

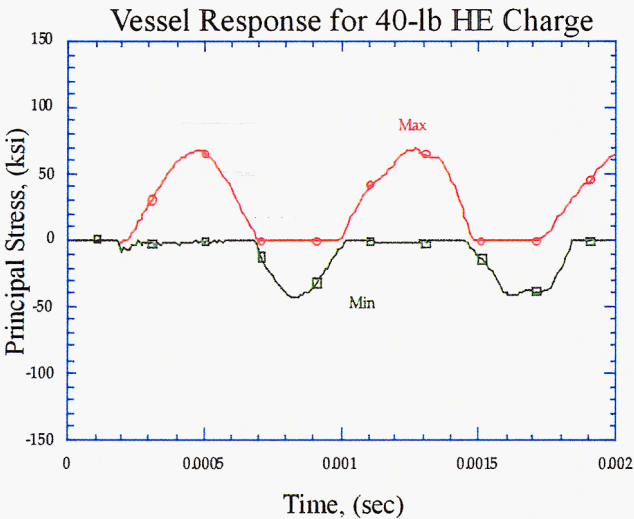


Figure 10. Principal Stress-Time History During Transient (2-ms)

This topic has been studied by Cooper [11], who observed:

Energy-Controlled Conditions. *It is poor practice to apply criteria developed for load-controlled conditions to energy-controlled conditions when deformations do not have to be controlled; and as was cited earlier, it is not the intent of Appendix F to limit deformations. If the condition is energy-controlled, the structural acceptance criteria should be related to the structural energy absorption. The only way to achieve that objective is to present the criteria in terms of strain limits which are proportional to the usable ductility of the material under the imposed stress state.*

Cooper also provided a technical basis for appropriate strain limits. That basis will be covered in the next sub-section.

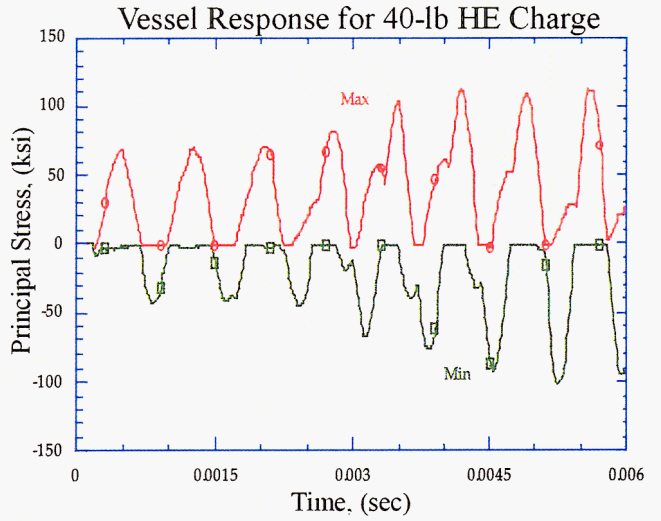


Figure 11. Principal Stress-Time History (6-ms)

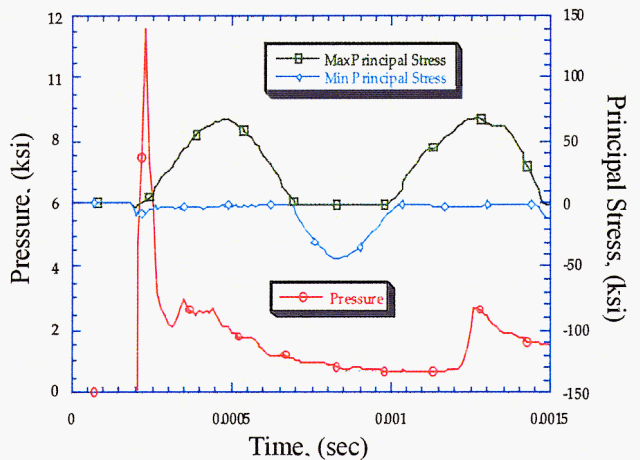


Figure 12. Pressure And Principal Stresses Superimposed

5.2 Energy-Controlled Membrane Strain Limits

The plastic tensile instability failure mechanism applies to a tensile membrane state of stress in the spherical shell portion of the vessel. ASME Code Section III, Paragraph NB-3213.26 and Appendix F discuss the use of this method for structural members under

predominantly tensile loading, where unbounded plastic deformation may occur. The plastic tensile instability load is the load at which the true stress of the material increases faster than can be accommodated by strain hardening.

The instability criterion is based upon the maximum through-thickness plastic strain at onset of plastic tensile instability. This criterion is imposed because of its direct applicability to strain-based (or deformation-controlled) methods. Following Cooper [11], in terms of true stress and true strain, the instability condition is governed by:

$$\frac{d\sigma}{d\varepsilon} = \sigma \quad (1)$$

A power-law representation of the material's true stress-strain behavior is assumed, where K is a constant and n is the hardening exponent. This is represented as:

$$\bar{\sigma} = K\bar{\varepsilon}_p^n \quad (2)$$

Substituting Eq. (1) into Eq. (2), the limiting strain at onset of instability for a uniaxial tensile specimen is derived as:

$$\bar{\varepsilon}_p = n \quad (3)$$

The effective (or equivalent) plastic strain, $\bar{\varepsilon}_p$, for a sphere under purely static internal pressure, at onset of collapse is:

$$\bar{\varepsilon}_p = \frac{2n}{3} \quad (4)$$

The instability criterion provides an upper bound on the circumferential and meridional plastic strains. Applying the instability criterion to the principal in-plane plastic strain for a sphere under internal pressure, the limit becomes:

$$\varepsilon_p = \frac{n}{3} \quad (5)$$

where ε_p = principal in-plane plastic strain.

This limit defines tensile instability for a spherical shell under static pressure conditions. The theory behind this limit can be found in Cooper [12] and Hill [13]. The theory specifically relates static internal pressure to the instability strain for ductile materials. Similar results can be derived for pressurized cylinders. Table 1 shows that, for "load-controlled" systems, e.g., systems that are loaded by direct static internal pressure, the plastic tensile instability strain is well characterized by the limits shown for the appropriate geometries.

Table 2, on the other hand, shows limits on "deformation-controlled" systems that are much higher than load-controlled limits. This is consistent with Code philosophy, whereby a higher stress allowable is applied for "secondary" stresses.

The implication of these two tables is that energy-controlled strain distributions are considerably different than load-controlled strain distributions, and resist failure in a more tolerant manner as a result of the distribution of those strains.

Table 1
Plastic Instability Condition (Load-Controlled)

Quantity	Tensile Specimen	Pressurized Cylinder	Pressurized Sphere
Effective strain	n	$\frac{\sqrt{3}n}{3}$	$\frac{2n}{3}$
Hoop strain	NA	$\frac{n}{2}$	$\frac{n}{3}$

Table 2
Plastic Instability Condition (Deformation-Controlled)

Quantity	Tensile Specimen	Cylinder	Sphere
Effective strain	n	n + 0.15	n + 1
Hoop strain	N A	$\frac{\sqrt{3}}{2}(n + 0.15)$	$\frac{(n + 1)}{2}$

5.3 Energy-Controlled Ductile Tearing Limits

The limits on plastic tensile instability, as shown in Tables 1 and 2, are associated with burst-type failure of the vessel in a biaxial membrane state of tensile stress, away from nozzles and other stress concentrations. These limits can be thought to be analogous to the **membrane stress** limits of the ASME Code. For locations in the vessel under more complex states of stress, ductile failure occurs by the mechanism of ductile tearing, which depends on the triaxiality of the local state of stress. Table 3 shows limits for the initiation of ductile tearing, where the effects of biaxial or triaxial tensile stress are very important. Values of the ratio of effective failure strain to uniaxial tensile failure strain ($\bar{\epsilon}_f / \epsilon_t$), as described by

$$\frac{\bar{\epsilon}_f}{\epsilon_t} = \frac{\sinh\left[\frac{\sqrt{3}}{3}(1-n)\right]}{\sinh\left[\frac{\sqrt{3}}{3}(1-n)TF\right]} \quad (6)$$

are indicated in Table 3 for selected geometries. TF, the Triaxiality Factor in Eq. (6), is

$$TF = \frac{\sigma_1 + \sigma_2 + \sigma_3}{\sigma_e} \quad (7)$$

where $\sigma_1, \sigma_2, \sigma_3$ = Principal stresses, and σ_e = Effective (or equivalent) stress, or

$$\sigma_e = \frac{1}{\sqrt{2}} \left[(\sigma_1 - \sigma_2)^2 + (\sigma_2 - \sigma_3)^2 + (\sigma_3 - \sigma_1)^2 \right]^{1/2} \quad (8)$$

In Table 3, the term $\frac{\bar{\epsilon}_f}{\epsilon_t}$ is the ratio of effective failure strain to uniaxial (tensile) failure strain ratio.

Figure 13 shows the triaxiality effect on failure strain for different values of the strain-hardening exponent. McClintock [14] derived the criterion from deformation solutions of elliptical holes in viscous materials. McClintock's ductile fracture criterion is based on void

nucleation, growth, and coalescence. Ju and Butler [15] further reviewed the criteria, incorporating actual material test data for 12 different ductile metals that were obtained from Westinghouse Reactor Division. This work was performed in support of the Clinch River Breeder Reactor program to address stress triaxiality concerns in the high temperature coolant loops.

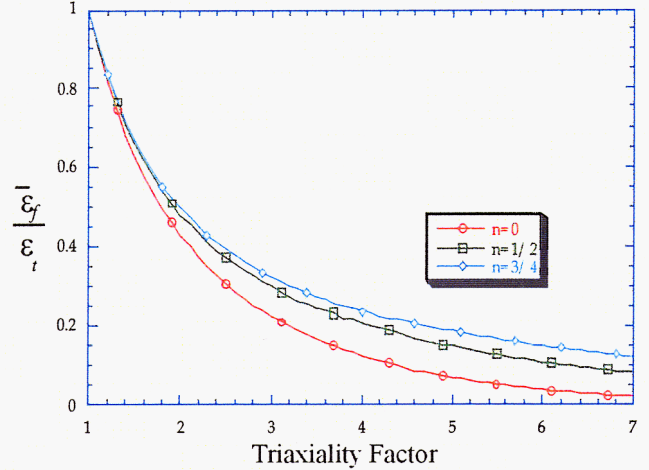


Figure 13. Triaxiality Effect On True Fracture Strain

The triaxiality factor for a sphere under internal pressure is 2. Figure 14 shows the LANL vessel material-specific strain-hardening exponent with the triaxiality correlation. The true fracture strain to uniaxial failure strain ratio is about 0.45 for the LANL vessel/material, where the true uniaxial fracture strain is:

$$\epsilon_t = \text{True Fracture Strain} = \ln\left(\frac{A_o}{A_f}\right) = \ln\frac{1}{1 - \frac{RA}{100}} \quad (9)$$

where RA is the Reduction in Area of a uniaxial tensile test specimen at failure. For the LANL spherical vessel manufactured from HSLA-100, the reduction of area and therefore the true uniaxial strain at failure is: RA=75%, $\epsilon_t = 1.386$.

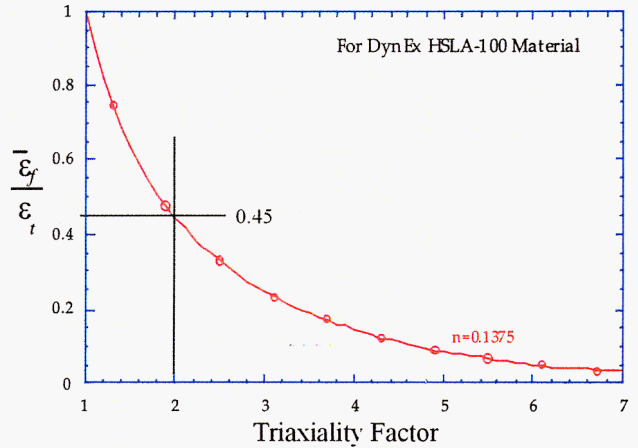


Figure 14. Triaxiality Factor For HSLA-100 Spherical Vessels

Table 3
Ductile Tearing Strain Parameters for Typical Geometries

Quantity	Tensile Specimen	Pressurized Cylinder	Pressurized Sphere
TF	1.0	$\sqrt{2}$	2.0
$\frac{\bar{\epsilon}_f}{\epsilon_t}$	1.0	0.68	0.44

NOTE: Based upon $n = 0.14$, which is typical of HSLA-100.

Table 4
Strain Limit Recommendations for Energy-Controlled Systems

Quantity	Basis	EPRI [11]	HSLA-100
Membrane Strain	Plastic Tensile Instability	$0.7Zn$	0.065
Peak Strain	Initiation of Ductile Tearing	$0.7\bar{\epsilon}_f$	0.44

Table 5
Conservative LANL Strain Limit Recommendations for Energy-Controlled Systems

Quantity	EPRI [11]	LANL
Membrane Strain	$0.7Zn = (0.065)$	$0.2\% = (0.002)$
Peak Strain	$0.7\bar{\epsilon}_f = 0.44$	$3\left(\frac{n}{3}\right) = 0.14$

Cooper [11] recommends that the membrane and ductile tearing peak strain limits shown in the third column of Table 4 be applied to energy-controlled systems, where, Z = Ratio of effective strain at maximum load $\bar{\epsilon}_{max}$, to strain-hardening exponent n . Using material parameters for the LANL vessel (i.e., HSLA-100 material), results are shown in the fourth column.

It should be noted that the 0.7 factor in the third column reflects margins on structural capacity to absorb energy for unexpected loads; i.e., the 1.43 margin represented by the 70 % is the same as that in Section III, Appendix F for load-controlled situations. The range of possible values for Z depends on the ratio of hoop-to-longitudinal stress. For the spherical vessel considered here, a value of 0.667 is assumed based upon biaxial tension state of strain. Furthermore, if no plastic instability analysis is performed, it is permissible to use a value of $Z=0.5$, according to Cooper [11]. Even with this coefficient, the lower-limit value of the membrane strain limit for energy-controlled structures is 0.033-in/in. Reference 10 chose a more conservative membrane plus bending strain limit associated with load-controlled conditions (see Table 1), using an effective plastic instability failure strain limit at $n/3$, which is indicative of a static pressure condition. This constitutes an implied safety factor of 2 for the design.

Therefore, for the combination of pure membrane (i.e., uniform through-thickness strains) and bending response of the vessel that occurs during the vessel's high-frequency vibration response from inertial effects, the allowable equivalent plastic strain is limited to one-half the effective plastic strain to cause failure for a spherical shell. From Eq. (5):

$$\bar{\epsilon}_p = \frac{n}{3} = 0.0467 \text{ in./in.}$$

where n = strain-hardening exponent and $n = 0.14$ (for HSLA-100). Note that this strain limit is similar to the static analysis based 5 % strain limit cited in KD-240(b)(1) of Section VIII, Division 3 of the ASME Code. In that case, it must be shown that at least a margin of 2 is available against that strain limit at every point in the vessel, based upon elastic, perfectly-plastic analysis with essentially no strain hardening.

Also, combined membrane, bending, deformation-controlled strains, and peak effects from strain concentrations, such as those near a nozzle to shell junction, are subject to the peak ductile tearing strain limit. These are considered highly localized strains, do not extend through-thickness, and are very short-lived. The allowable equivalent plastic strain for this condition will be limited to three times the membrane limit:

$$\bar{\epsilon}_p = 3\left(\frac{n}{3}\right) = 0.14 \text{ in./in.}$$

This peak strain limit is well above the 5 % limit in KD-240(b)(1), especially considering the marginal requirement of a factor of 2. There is a need to reconcile the Section VIII Division 3 static collapse pressure strain limits with those cited here.

The three plastic strain limits, uniform membrane, membrane and bending, and complex strain field, are applied throughout the vessel

system. Note that equivalent plastic strains are cumulative over time, as calculated in the numerical models. This is a particularly convenient approach because the analyst need only compare the last time step equivalent plastic strain with the appropriate strain limits. In comparison with the energy-controlled criterion described by Cooper [11], the allowable strain limits from Reference 10 are very conservative, as shown in Table 5.

6. SUMMARY

The use of containment vessels to mitigate the effects of high explosive reaction products and hazardous material release is of utmost importance in several areas. Because of the different types of loading experienced in a containment vessel, the methods of analysis and certification are slightly different. Dynamic impulse loading, associated with HE detonation, followed by long-term residual quasi-static pressure loading, must be treated differently during design. Whereas an appropriate analysis and certification method might be the ASME Code, Section VIII, Division 1, certain conditions are currently not covered.

Two methods have been discussed herein, (1) AWE methodology using Section VIII, Division 3, for multiple-use HE loading and, (2) LANL methodology for single-use applications. The latter methodology uses a combination of Section VIII, Division 1 for the residual static pressure, coupled with a modified plastic tensile instability methodology drawn from Section III, Division 1, Appendix F. In this methodology, allowable plastic strain limits are imposed for (a) pure through-thickness membrane loads and (b) complex states of strain.

7. REFERENCES

- [1]. T. A. Duffey and E. A. Rodriguez, "Dynamic Vs. Static Pressure Loading in Confinement Vessel," DYNEX-00-084, DynEx Vessel Project, Los Alamos National Laboratory, Los Alamos, NM, November 20, 2000.
- [2a]. A. M. Clayton, "Hydrodynamics Research Facility - Design Methods Used for AWE Containment Vessels", Welding Research Council Progress Reports, Volume LVI, No. 11/12, pp. 6-28, November/December 2001.
- [2b]. A. M. Clayton, "Design Methods Used for AWE Containment Vessels," File AWE/DSD/C/750.6.2/AC/001, Hydrodynamics Research Facility, Atomic Weapons Establishment, Aldermaston, United Kingdom, May 4, 2000.
- [3]. W. E. Baker, Explosions in Air, 2nd Edition, WE Baker Engineering, San Antonio, TX, 1983.
- [4a]. ASME Boiler & Pressure Vessel Code, Section III, Division 1, Non-Mandatory Appendix F, "Rules for Evaluation of Service Loadings with Level D Service Limits," ASME International, New York, NY, July 2001.
- [4b]. ASME Boiler & Pressure Vessel Code, Section III, Division 1, Mandatory Appendix II, "Experimental Stress Analysis," ASME International, New York, NY, July 2001.

- [5]. R. E. Nickell, "Nonlinear Dynamics by Mode Superposition," *Computer Methods in Applied Mechanics and Engineering*, Volume 7, No. 1, pp. 107-129, January 1976.
- [6]. J. C. Gerdeen, "A Critical Evaluation of Plastic Behavior Data and a Unified Definition of Plastic Loads for Pressure Components," in: *Welding Research Council Bulletin 254*, pp. 1-64, Welding Research Council, New York, NY, November 1979.
- [7]. P. S. Symonds and J. M. Mosquera, "A Simplified Approach to Elastic-Plastic Response to General Pulse Loads," Paper No. 84-WA/APM-52, ASME Winter Annual Meeting, New Orleans, LA, December 9-14, 1984.
- [8]. ABAQUS/Standard Users Manual, Hibbitt, Karlsson, and Sorensen (HKS), Providence, RI., 2001.
- [9]. R. E. Nickell, R. Sauve, and W. Teper, "Buckling Design Analysis for Impact Evaluation," *Transactions ASME, Journal of Pressure Vessel Technology*, Volume 107, No. 2, pp. 165-171, May 1985.
- [10]. C. Romero, "DYNEX Standard for Construction of HSLA-100 Confinement Systems," DYNEX-01-23, DynEx Vessel Project, Los Alamos National Laboratory, Los Alamos, NM, June 27, 2001.
- [11]. W. E. Cooper, "Rationale for a Standard on the Requalification of Nuclear Class 1 Pressure-Boundary Components," *Electric Power Research Institute, EPRI Report No. NP-1921*, Prepared by Teledyne Engineering Services, October 1981.
- [12]. W. E. Cooper, "The Significance of the Tensile Test to Pressure Vessel Design," *Welding Research Council, WRC Supplement, Pressure Vessels*, January 1957.
- [13]. R. Hill, "A Theory of Plastic Bulging of a Metal Diaphragm by Lateral Pressure," *Philos. Mag.*, Vol. 41, No. 7, pp.1133-1142, 1950.
- [14]. F. A. McClintock, "A Criterion for Ductile Fracture by Growth of Holes," *Transaction of the ASME, American Society of Mechanical Engineers*, pp. 363-371, June 1968.
- [15]. F. D. Ju and T. A. Butler, "Review of Proposed Failure Criteria for Ductile Materials," *Nuclear Regulatory Commission, NUREG/CR-3644*, April 1984.